

Declustering and Debiasing

M. J. Pyrcz (mpyrcz@ualberta.ca) and C. V. Deutsch (cdeutsch@ualberta.ca)

Centre for Computational Geostatistics
University of Alberta, Edmonton, Alberta, CANADA

Abstract

Strategic project decisions are based on the distributions global variables, for example, total mineable resource, or recoverable oil volume. These global variables distributions are very sensitive to rock type proportions and the histograms of continuous variables. Representivity of the input one point statistics is important in all spatial models.

The process of assembling representative one point statistics is complicated by sample clustering and spatial bias in the data locations. Explanation is provided on the source of nonrepresentative sampling and the need for declustering and debiasing. This work addresses some key implementation details on declustering. Standard declustering is not always able to correct for sampling spatial bias. Two methods for correcting bias in the one point statistics: “trend modeling for debiasing” and “debiasing by qualitative data” are reviewed and demonstrated with a poly metallic data set.

Introduction

Great computational effort is exerted to build realistic geostatistical simulation models. The goodness of these models is judged by their ability to reproduce input one-point statistics and continuity structures. Geostatistical techniques slavishly reproduce input lithofacies proportions and the histogram of petrophysical properties (Gringarten et al., pg. 1, 2000). There is very little intrinsic declustering or debiasing within geostatistical simulation algorithms. Geostatistical simulation always weights the input distribution. Gaussian simulation in particular ensures that the input distribution is approximately reproduced. Clustered sampling that misrepresents the proportions within specific bins, or spatial bias sampling that does not characterize the full range of the distribution, in the input distributions must be dealt with explicitly.

The importance of representative input distributions must be evaluated with respect to the sensitivity of the response variable to clustering or bias in the input statistics. Simulated models are only an intermediate result. Management decisions focus on the results after the application of a transfer function.

Declustering methods are commonly applied in an automated fashion. This work addresses the properties of a variety of declustering algorithms and methods of improving application. Issues such as working with anisotropy, within facies and with multiple variables are addressed. It is essential to understand the applicability and limitations of declustering algorithms since blindly applying declustering may be worse than working with the naïve statistics.

Declustering is ineffective in cases with spatial bias. Debiasing tools such as “trend modeling for debiasing” and “debiasing by qualitative data” should be brought into common practice for the purpose of improving the inference of the one point statistic.

Nonrepresentative Sampling

It is natural that spatial data are collected in a nonrepresentative manner. Preferential sampling in interesting areas is intentional and facilitated by geologic intuition, analogue data and previous samples. This practice of collecting clustered or spatially biased spatial samples is encouraged by technical and economical constraints, such as future production goals, accessibility and the costs of laboratory work.

The cost of uncertainty is not the same everywhere in the area of interest. For example, the cost of uncertainty within a high grade region is much higher than the cost of uncertainty within clearly waste

material. Good delineation and a high level of certainty within the high grade materials allows for accurate reserves estimation and optimum mine planning.

Future production goals may also encourage clustered or spatially biased sampling. It is common to start mining in high grade regions. In this case it is desirable to delineate and characterize the high grade regions.

Practical issues of accessibility can also cause spatially biased sampling. For example, the drilling depth or available drilling stations may constrain sample selection. In the presence of a vertical trend, limited depth of drilling may result in a subset of the underlying distribution not being sampled. There are many possible scenarios under which accessibility would be a concern (see Figure 1).

Nonrepresentivity may also be introduced at the assaying stage. For example, when removing sections of core for the purpose of permeability measurement, it is unlikely that a section of shale would be subjected to expensive testing. Likewise, barren rock may not be sent for assays.

Conventional Statistics

Conventional statistics do not provide reasonable solutions to the problem of constructing representative spatial distributions. A simple random sample from the population of interest would be representative, but inappropriate in most cases. A sample is said to be representative when each unit of the population has the same probability of being sampled. In conventional statistics this is accomplished by avoiding preferential sampling or opportunity sampling. As explained above, there are many reasons that geologic samples are collected in a biased manner.

Regular or random stratified sampling may be able to provide a good approximation of a representative distribution. Sampling on a regular grid is rarely practical for the same accessibility and economic reasons stated above. Regular sampling grids may be applied in preliminary resource investigation. These sampling campaigns are often augmented by nonsystematic infill drilling. One approach would be to omit the clustered infill samples for the purpose of building distributions. While this would more closely agree with conventional statistical theory, throwing away expensive information is not very satisfying (Isaaks and Srivastava, pg. 237-238, 1997).

Declustering

Declustering is well documented and widely applied (Deutsch, pg. 53-62, 2001; Isaaks and Srivastava, pg. 237 – 248, 1997; Goovaerts, pg. 77-82, 1997). There are various types of declustering methods, such as cell, polygonal and kriging weight declustering. These methods rely on the weighting of the sample data, in order to account for spatial representivity. Figure 2 shows the effect of weighting the histogram. Note that weighting does not change the values: only the influence of each sample is changed.

There are two important assumptions in all declustering techniques: (1) the entire range of the true distribution has been sampled or the data is not spatially biased, and (2) the nature of the clustering is understood. Declustering may not perform well without these assumptions. The first assumption is required since the weighting only adjusts the influence of each sample on the distribution and does not change the actual sample value. Figure 3 shows an example where declustering could not work; there are no low samples to give more weight to.

The second assumption is that the nature of the clustering is understood. If the data have no spatial correlation, there would be no reason to apply declustering. Each sample, regardless of location, would be a random drawing from the underlying distribution. Without an understanding of the spatial nature of the data, declustering may be incorrectly applied.

There are a variety of methods to calculate the declustering weights. Polygonal, cell and kriging weight methods will be discussed.

Polygonal Declustering

Polygonal declustering is commonly applied in other scientific disciplines, such as hydrology, for the purpose of correcting for clustering in spatial data. The method is flexible and straightforward. The

polygonal declustering technique is based on the construction of polygons of influence about each of the sample data. These polygons of influence are described by all midpoints between each neighbouring sample data. Simple example data set with polygons of influence is shown in Figure 4.

For each polygon of influence the area is calculated and the weight assigned to each sample is calculated as the proportion of polygon area to the entire area of interest (same as the sum of all polygon areas).

$$w'_j = \frac{area_j}{\sum_{j=1}^n area_j} \cdot n$$

where n is the number of data.

Polygonal Declustering Sensitivity to Boundary

The area associated to peripheral samples is very sensitive to the boundary location. If the boundary is located far from the data, then the peripheral samples will receive a large amount of weight, since the area of their polygons of influence increase.

In general this great sensitivity to the boundary is perceived as weakness in polygonal declustering. A common technique is to simply apply the boundary of the area of interest. This may be defined by geology, leases etc. This approach may be reasonable depending on the problem setting. The second technique is to assign a maximum distance of influence to the samples.

Polygonal Declustering Approximation

The application of polygonal declustering to a 3D data set requires the calculation of complicated solid boundaries and volumes, which is computationally expensive. A close approximation can be rapidly be calculated by discretizing the area of interest into a fine grid and assigning each node to the nearest data.

Polygonal Declustering and Anisotropy

Directional weights may be applied to the polygonal declustering algorithm in order to account for anisotropy. This is demonstrated in Figure 5 for anisotropy ratios of 1, 2, 5, and 10:1.

Cell Declustering

The cell declustering technique is the most common method applied in Geostatistics. It is insensitive to the boundary locations and for this reason is seen as more robust than polygonal declustering. A cell declustering algorithm, DECLUS is standard in GSLIB.

Cell declustering applies the following steps:

- for each origin offset
 1. overlay a regular grid over the data
 2. assign an intermediate weight of the reciprocal of the number of data in the cell
 3. standardize the weights by dividing by the number of cells with data
 4. shift the grid
- average resulting weights over each origin offset

The method is demonstrated in Figure 6 for one origin offset.

For a given cell the weight of each sample is calculated as follows,

$$w'_j = \frac{\frac{1}{n_i}}{\text{number of cells with data}} \cdot n$$

where n_i is the number of samples in the cell in which sample j is located and n is the total number cells with samples.

Cell Declustering and Cell Size

The weights assigned by cell declustering are sensitive to the cell size. If the cell size is set as very small then every sample occupies its own cell and the result is equal weighting or the naïve sample distribution. If the cell size is set as very large then all samples reside in the same cell and the result is once again equal weighting.

A specific cell size will result in an unique set of weights. The question is, ‘which cell size identifies the best weights?’. If there is a coarse grid with additional infill sampling then the coarsest sample spacing is the best cell size (see Figure 7)

If this configuration is not present then a common procedure is to assign the cell size, which maximizes or minimizes the declustered mean. This is demonstrated in Figure 8. This procedure is applied when the samples are clearly clustered in low or high values (apply the cell size which renders the maximum or minimum declustered mean respectively). The results are only accurate when there is a clear minimum or maximum. One should not blindly assign the minimizing or maximizing cell size. It is shown in the next section that such an assignment may results in poorer results than the naïve distribution in expected value.

Cell Declustering with the Minimizing and Maximizing Cell Size Warning

A large number of runs were carried out to determine whether in expected terms the minimum or maximum result in an acceptable declustered mean (a declustered mean which closely approximates the true underlying mean). 101 realizations were generated by sequential Gaussian simulation of a 50 x 50 space. The continuity range was selected as small (range of 10) with respect to the simulation size so that the realization mean and variance were consistently near 0.0 and 1.0 respectively (minimal ergodic fluctuations). Regular samples were taken at 10 unit spacing and then infill samples were taken around a specific percentile data value. By changing the specific percentile the level of clustering was changed.

The expected true mean, sample mean, 9 cell size, 10 cell size and minimum or maximum cell size were compared for each percentile (see Figure 9). For cases with a percentile near the median (low magnitude of clustering), application of the minimizing or maximizing cell size resulted in poorer results than the naïve sample mean. The application of the coarsest regular sample spacing resulted in a best declustered mean in expected terms. This confirms that there is a problem, in expected terms, with systematically applying the cell size with min/max declustered mean, and that knowledge of the appropriate cell size provides better results in expected terms.

Cell Declustering and Origin Offsets

Cell Declustering weights are also sensitive to the grid origin. To remove this sensitivity the procedure is repeated with a specified number of origin offsets and the results are averaged.

The application of origin offsets has the following practical impacts:

1. smoothes out steps that would occur in the declustered mean and cell size relationship.
2. makes large cells sizes ($> \frac{1}{2}$ data set size) unreliable

These effects are demonstrated by an exercise. Cell declustering was applied to the simple data set with a variety of origin offsets. Figure 10 shows the smoothing effect of the application of origin offsets. The

greater the number of offsets the smoother the relationship between declustered mean and cell size. Also, it can be seen that offsets cause the results to be unreliable when large cell sizes are applied. The data set dimensions are 10x5 units. It would be expected that at a cell size of 10 that the declustered mean would be equal to the naïve mean. With offsets this does not occur. The cause is demonstrated in Figure 11.

This reinforces the rule of thumb:

- Calculate the declustered mean for cells sizes 5% to 50% of the size of the area of interest and apply the minimum number of offsets required to get a reasonably continuous relationship (around 5 is usually sufficient).

Cell Declustering with Multiple Variables

The common practice is to apply cell declustering to the primary variable and apply these weights to all other collocated variables. This is intuitive since clustering should be related only to the data locations, not the data values. If the cell size is chosen based on the declustered mean and cell size relationship, this practice may be questioned since the declustered mean is dependent on the data values. Will the maximizing or minimizing cell size be the same for each variable?

To explore this issue an exhaustive data set was generated with three collocated and correlated standard normal variables. Table 1 below lists the properties of each variable.

	Variogram Range	Correlation to Var. 1
Variable 1	10	-
Variable 2	20	0.7
Variable 3	5	-0.8

Table 1 – Properties of the three correlated variables.

Samples (50) were drawn from the exhaustive data sets, and the sample variograms and correlations were checked (see Figure 12). The sampling scheme was based on coarse grid (20 unit spacing) with some infill clusters and random samples. The relationships of declustered mean vs. cell size are shown in Figure 13.

For all three variables there is a clear maximum or minimum at the same cell size. This has occurred despite different variograms, and correlations. This exercise has supported the current practice of applying the same cell declustering weights to all collocated variables.

Kriging Weight Declustering

Another technique applied for calculating declustering weights is to perform a kriging of the area of interest and to sum the weights applied to each conditioning data and then to standardize these sums. This is analogous to block kriging the area of interest.

This technique is similar to polygonal declustering in that it is sensitive to the boundaries. In addition, this method is sensitive to search parameters. This method also integrates information on the spatial continuity of the population, through the variogram. Since kriging weight declustering is a discretized approximation method, the approximation improves as resolution of the kriged grid increases.

Disadvantages of Kriging Weight Declustering

In general, this approach is much more computationally intensive than the polygonal and cell declustering techniques. Also, there may be artifacts in the weights due to the string effect. This string effect is illustrated in Figure 14.

The conditioning data at the extents of the string receive greater weight. For the peripheral data the weighting is greater, even at locations much closer to other data. This is caused by the implicit assumption of kriging that area of interest is imbedded in an infinite domain.

Kriging Weight Declustering and Negative Weights

It is appropriate to include negative weights when calculating the sum of weights. It is possible that this would result in a negative declustering weight. One way in which this would be realized would be if the conditioning data is outside the area of interest and it is screened. In general, the conditioning data are within the area of influence and a negative declustering weight would not occur.

Declustering and Anisotropy

Cell, polygonal and kriging weight declustering may be configured to account for anisotropy in the data. An aspect ratio may be applied to the cells, the distance measure may be weighted in polygonal declustering and anisotropic variograms may be applied in kriging weight declustering.

An example cross section is shown in Figure 15. There is a large horizontal to vertical anisotropy continuity ratio. Wells with sample locations are added to the cross section (see Figure 16). Isotropic declustering would assign similar weights to the samples in all three drill holes, since they are all nearly equally spaced. Yet our knowledge of the spatial continuity tells us that the samples in drill hole 2 are more redundant. Also, without accounting for anisotropy sample A in Figure 17 would receive greater weight. Considering the high level of anisotropy this would not be correct. These cases can be addressed by applying anisotropy to the declustering method.

Declustering and the Boundary

The cell technique is unique in that it does not consider the boundary. This is indicated as a strength, since this results in a more robust assignment of declustering weights. While this is true, this may result in some pathological problems.

It may not be reasonable to ignore the boundary in assigning weights to the example data set (see Figure 18). Clearly although the data is equally spaced it is not equally representative of the area of interest. Figure 18 illustrates the differences between cell, polygonal and kriging weight declustering in assigning declustering weights.

Cell declustering assigns equal weights to the data since it does not consider the boundary, while polygonal and kriging weight declustering account for the boundary location. Also, kriging weight declustering shows some artifacts due to screening in this case. Note that the data in the second row from the bottom receive less weight due to screening.

Declustering Within Rock Types

A common procedure is to model each rock type's properties separately and then to simulate continuous variables (such as grade) within each rock type. A simple example is shown in Figure 19. This cross section indicates two separate tabular facies sampled by two complete drill holes.

In this setting representative distributions of each rock type would be constructed by separating area of interest into distinct rock types. Then weights would be applied to the naïve distributions for each rock type. Figure 20 illustrates the separation of the area of interest into separate rock types.

In this setting the boundary is very important. This would disqualify the application of cell declustering. When there are strings of data as shown in Figure 20 then the kriging weight declustering method suffers from increasing events of the string effect. In this example the data nearest the contact layers would receive disproportionate weight. Polygonal declustering is a good method to apply since sensitivity to the boundary is required, and the polygonal method would not suffer from any artifacts.

Polygonal Declustering Within Rock Types

To illustrate the application of polygonal declustering with a rock type model, a synthetic example was constructed. A random 2D data set was constructed with a uniform distribution in x and y and a normal Gaussian property. The rock type model was constructed by smoothing an unconditional sequential

indicator simulation with 4 categories (see Figure 21). Then conventional polygonal declustering was applied to the data set irrespective of the rock type (see of Figure 22} left for a map of declustered weights and the polygons of influence). Also, polygonal declustering was performed constrained by the rock types (see right of Figure 22) for the declustered weights and the polygons of influence. Considering the rock types significantly improves the declustering weights.

When the entire range of the distribution is not sampled then it is necessary to apply debiasing techniques.

Debiasing

There are two methodologies that may be applied to correct biased samples. The first method, “trend modeling for debiasing”, separates the variable into a trend and residual. The second approach, “debiasing by qualitative data”, corrects the distribution with a representative secondary data distribution and calibration relationship to the primary variable of interest.

In the presence of a clear and persistent trend, trend modeling may be applied to ensure that the correct distribution is reproduced. Trend modeling is well established (Goovaerts, pg. 126, 1997; Deutsch, pg. 182, 2001). The steps are as follows: (1) remove an appropriate trend model, (2) stochastically model residuals, and (3) replace trend a posteriori. The resulting models reproduce the trend. An advantage of this technique is that the simulation step may be simplified since cosimulation is not necessarily required. While this technique will often debias the distribution, there is no direct control over the resulting distribution. The result should be checked. Care should also be taken to build an appropriate trend model. This requires that the mean of the residuals is close to 0.0 and the correlation between the trend and residual is close to 0.0.

Another technique is to use soft data that is representative of the entire area of interest, and an understanding of the relationship between the primary and soft secondary data to correct the primary distribution (Deutsch et al., 1999). Then, this corrected distribution is applied as a reference distribution to the subsequent simulation of the primary variable. The underlying relationship between the primary and secondary data may be assessed from geologic modeling or the physics of the setting. This relationship may not be directly observed due to a lack of data; nevertheless, a relationship between the secondary and primary data, $\hat{f}_{x,y}(x,y)$ must be inferred for debiasing (see Figure 23).

The construction of the bivariate calibration is the difficult component of debiasing. There are a variety of techniques for building this distribution. For example, the program SDDECLUS by Deutsch relies on the user submitting data pairs which describe the bivariate relationship. This approach allows for the greatest flexibility, since there is no constraint on the form of the bivariate calibration. For each paired primary data a weight is assigned based on the secondary distribution

Another method is to calculate a series of conditional distributions of the primary given the secondary data, $f_{\text{primary}|\text{secondary}}$, over the range of observed secondary value. This can be extrapolated over the range of all secondary data by a trend. This is illustrated in Figure 24. The primary distribution is then calculated by scaling the binned bivariate calibration by the secondary distribution. For the above bivariate calibration this is illustrated in Figure 24. This is a discrete approximation of the solution of the secondary distribution as expressed in Equation 1.

$$f_y(y) = \int_x f_{y|x}(y|x) \cdot f_x(x) dx \quad (1)$$

The trend method indirectly corrects the global distribution. This leads to models with precise trend reproduction and indirect control over the distribution. The qualitative method focuses on directly correcting the global distribution and retaining consistency by applying the secondary data as collocated data in the simulation. The result is direct control over the reproduced distribution and indirect control over trend reproduction.

The two techniques, also differ in the information which is integrated into the numerical model. In the first method the simulation is augmented by information concerning the spatial behavior of the primary variable. The second method relies on information concerning a more representative secondary data and the relationship between the primary and secondary data. The information available may limit the ability to

apply either method. The method chosen also affects the resulting model of uncertainty. Each will potentially decrease the overall model uncertainty. This is expected since each option involves adding conditioning to the numerical model.

Debiasing Example

A realistic data set based on a 2D poly metallic “red” vein is presented. This sample set was gathered by drilling. Some data were removed for checking and illustrating the method. For the sake of comparison, an approximation of the true gold distribution was constructed by applying polygonal declustering to the complete “red” data set (see Figure 26). In the complete data set the entire area of interest is well delineated (see left of Figure 27 for location map of the complete data set) and polygonal declustering results in a reasonable distribution. Since the true underlying distribution is not available, this distribution will be assumed to be a good approximation of the underlying distribution.

There is a significant positive correlation between the gold grade and the thickness of the vein (correlation coefficient = 0.6), so it was decided to apply gold as the primary variable and a smooth kriged thickness map as the representative secondary data, see Figure 27.

Polygonal declustering was applied to the reduced data set. The resulting declustered distribution and the voronoi polygons are shown in Figure 28. There is a great difference between the underlying mean gold grade (0.69 g/t) and the declustered mean gold grade (1.25 g/t) and distributions do not have the same shape. There is additional information that could aid in the inference of the correct distribution, such as thickness that has a significant correlation to the primary variable, gold. There is also a clear trend in the gold grades. This analogue information improves the distribution.

Debiasing by Qualitative Data

Debiasing by qualitative data with a bivariate trend was applied to correct the gold distribution. The results are shown in Figure 29. The bivariate trend was set as a second order function with a linear segment for gold grades greater than 5.0 g/t. This density calibration table was weighted by the thickness (secondary) distribution, and the resulting corrected gold (primary) distribution is shown on the left of Figure 29. Any estimated negative grades were set to zero. Sequential Gaussian simulation (SGSIM) was performed with the debiased distribution as a reference distribution and the thickness map as a collocated secondary data. A correlation coefficient of 0.72, was calculated from the density calibration table, was applied to the secondary data. An omni-directional variogram with a nugget effect of 0.4 and an isotropic spherical structure with a range of 140 units was used to represent the gold spatial continuity. No effort was made to calculate and model a more specific variogram model since variogram inference is not a focus of this work. Three realizations are shown in Figure 30.

The strong correlation between the primary data and the collocated secondary data has resulted in a clear trend in the realizations. Some example simulated distributions are shown in Figure 31 and the distribution of the realization means for 100 realizations are shown in Figure 32. The average of the realization means is 0.84, which is higher than the average of the reference distribution (see Figure 26). Nevertheless, the resulting distribution is closer to the reference true distribution in shape and statistics than the declustering results.

Trend Modeling for Debiasing

Trend modeling for debiasing was also applied. A trend model was constructed from a moving window average of all the gold samples in the complete data set. This model was scaled such that the mean of the residuals was near 0. The gold samples, gold trend model and distribution of the residuals are shown in Figure 33. Sequential Gaussian simulation was performed with the residuals and the trend model was added a posteriori. Any negative estimates were set to 0. Three example realizations are shown in Figure 34. The trend is consistently reproduced in each realization. Some realization distributions are shown in Figure 35 and the distribution of the realization means for 100 realizations are shown in Figure 36. The mean of the realization means is 0.90. The resulting distributions are closer to the approximate true distribution in shape and mean than the declustering results.

Conclusions

Nonrepresentative sampling is unavoidable in most geologic settings. Declustering techniques are widely used and are generally effective for correcting for nonrepresentative data. It is important to understand the appropriate methods and settings for the application of declustering. In settings where the underlying distribution has not been adequately sampled, declustering may not be adequate and debiasing is required. Debiasing relies on analogue information such as a trend in the primary variable or a well sampled secondary variable and a calibration. Two debiasing methods, trend modeling for debiasing and debiasing by qualitative data, have been demonstrated with a mining data set.

Acknowledgements

We are grateful to the industry sponsors of the Centre for Computational Geostatistics at the University of Alberta and to NSERC and ICORE for supporting this research. Also, we would like to acknowledge Julian Ortiz who contributed to work on declustering.

References

- Deutsch, C.V. and A.G. Journel. 1998. *GSLIB: Geostatistical Software Library: and User's Guide, 2nd Ed.* New York: Oxford University Press.
- Deutsch, C.V., P. Frykman, and Y.L. Xie, 1999. Declustering with Seismic or "soft" Geologic Data, *Centre for Computational Geostatistics Report One 1998/1999*, University of Alberta.
- Deutsch, C. V., November 2001. *Geostatistical Reservoir Modeling*, in final stages of production at Oxford University Press,
- Goovaerts, P., 1997. *Geostatistics for Natural Resources Evaluation*. New York: Oxford University Press.
- Gringarten, E., P. Frykman, and C.V. Deutsch. December 3-6, 2000. *Determination of Reliable Histogram and Variogram Parameters for Geostatistical Modeling*, AAPG Hedberg Symposium, "Applied Reservoir Characterization Using Geostatistics", The Woodlands, Texas.
- Isaaks, E. H. and R. M. Srivastava. 1989. *An Introduction to Applied Geostatistics*, New York: Oxford University Press.

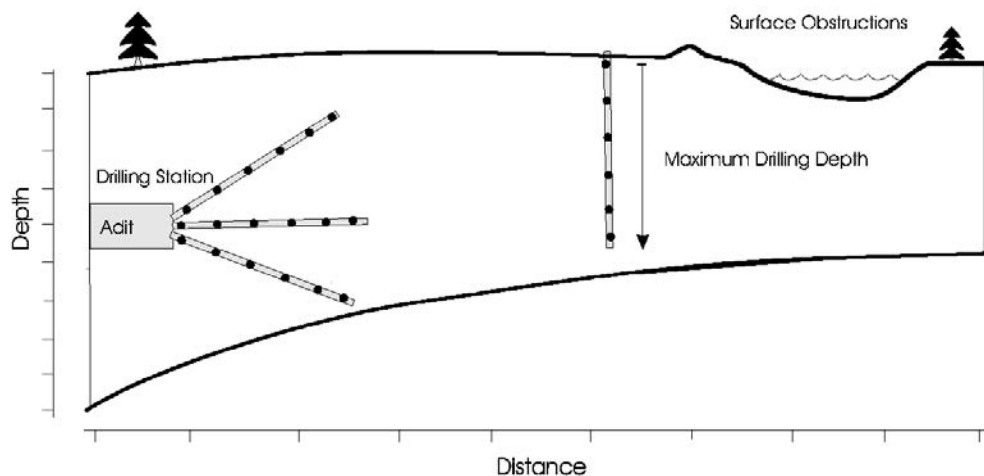


Figure 1 - Some examples of accessibility constraints illustrated on a cross section.

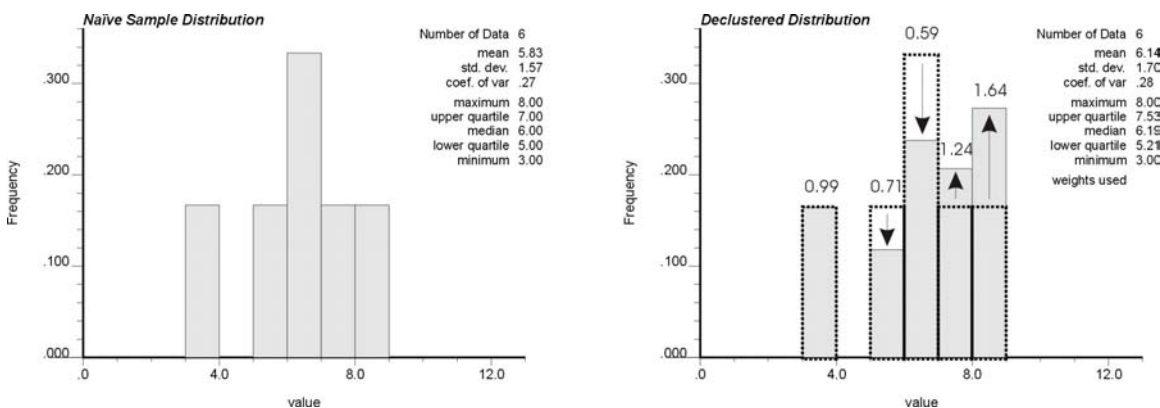


Figure 2 - The influence of weighting on a distribution. On the right the naïve distribution (dotted line) is superimposed on the declustered distribution with the weights indicated.

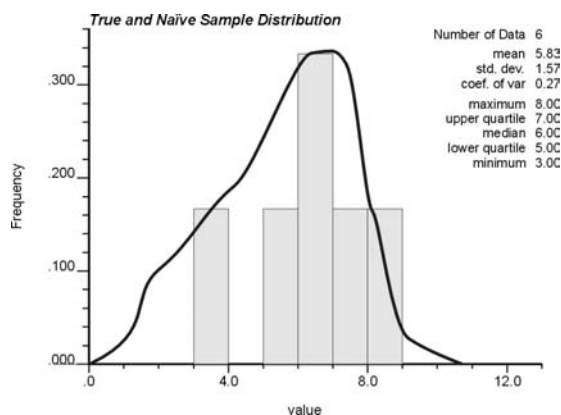


Figure 3 An example underlying distribution (bold line) and the sample distribution (histogram). The entire range of the true distribution has not been sampled.

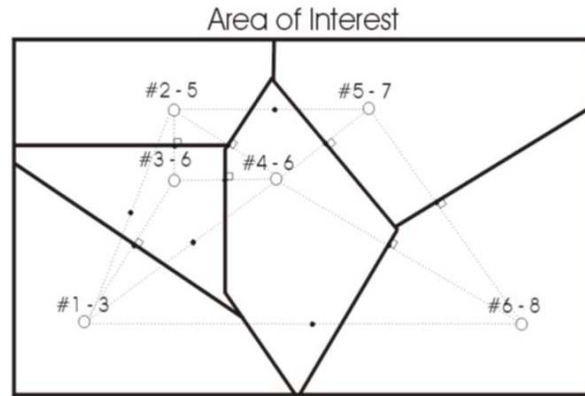


Figure 4 - The polygon of influence.

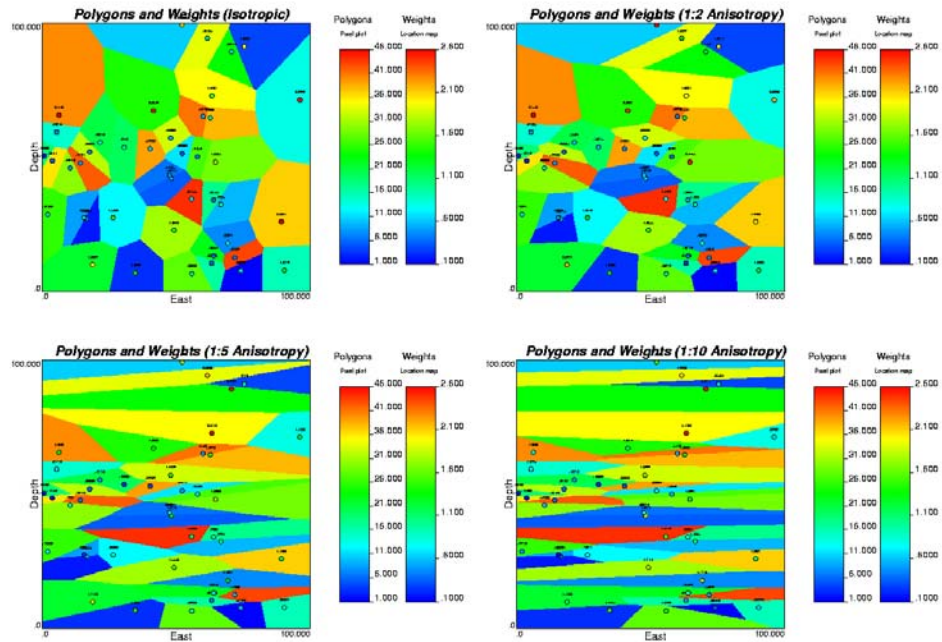


Figure 5 – The effect of anisotropy on the polygons of influence. The horizontal distance was weighted by factors 1, 2, 5, and 10.

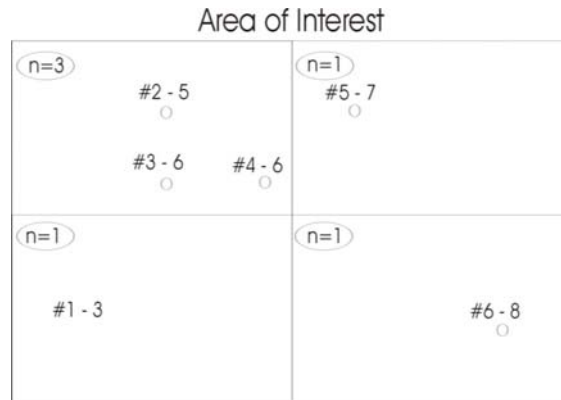


Figure 6 – A simple illustration of the cell declustering technique.

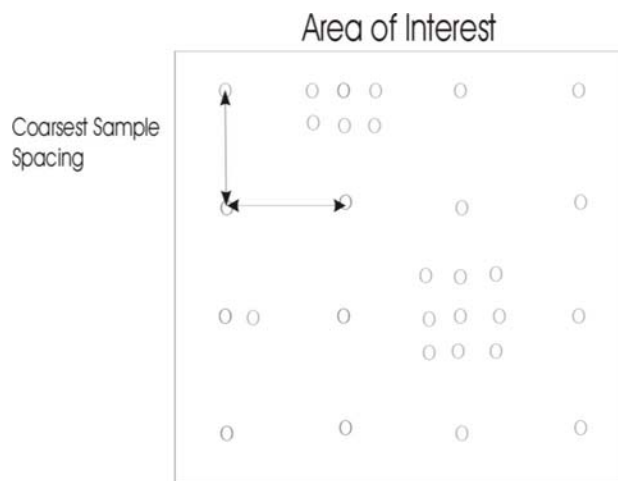


Figure 7 – Optimum Cell Size Assignment

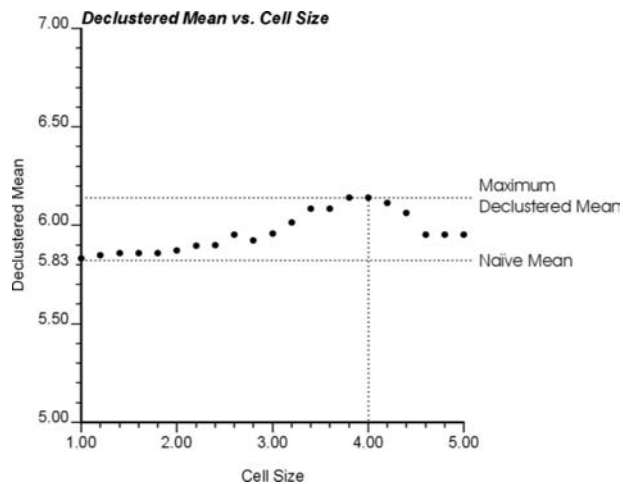


Figure 8 – The Relationship between Declustered Mean and Cell Size For the Simple Data Set

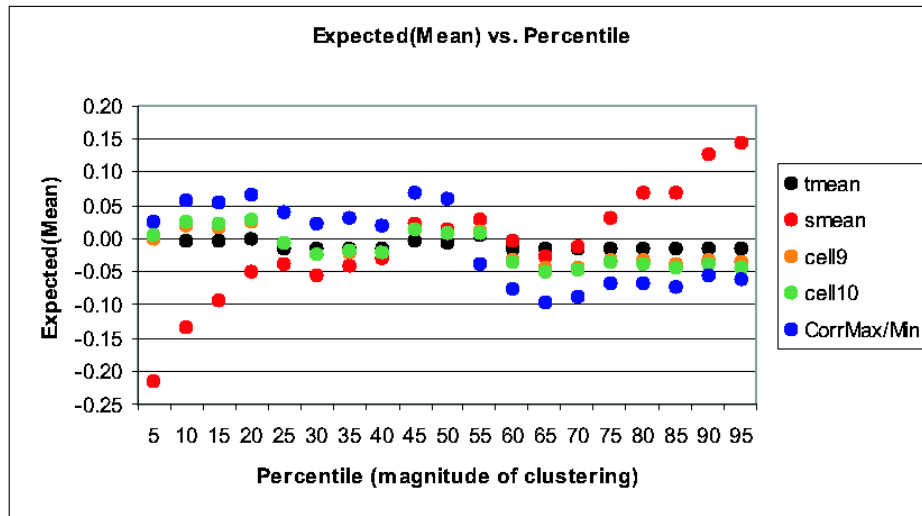


Figure 9 – A chart indicating the expected true, sample and declustered means (for cell size 9, 10 and minimizing or maximizing), vs. the percentile of clustering. The consistent application of the coarsest sample spacing as cell size results in a declustered mean closer to the true mean in expected terms.

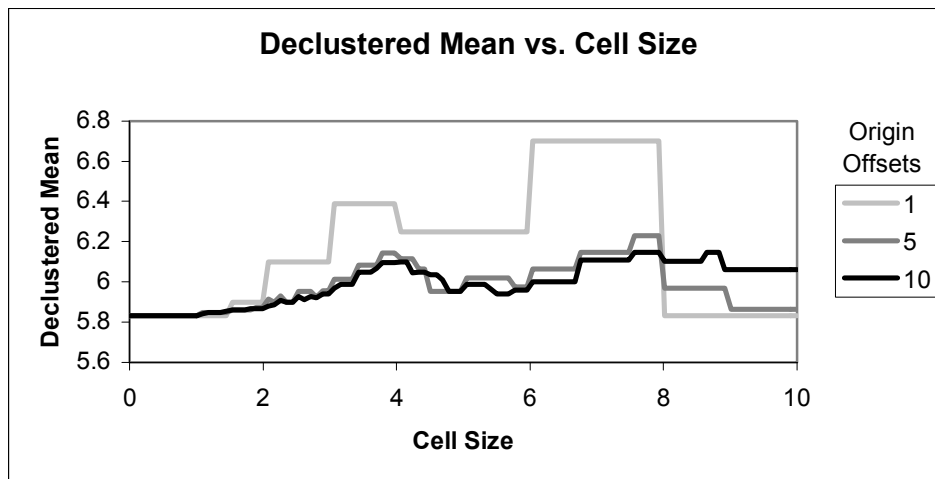


Figure 10 – The declustered mean vs. cell size relationship with a variety of origin offsets. Note that the offsets smooth out steps in the declustered mean and cell size relationship. Also, with origin offsets the declustered mean does not approach the naïve sample mean as the cell size becomes large.

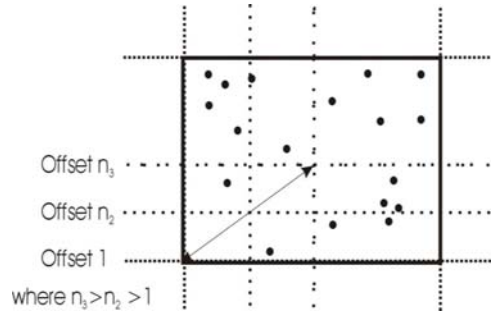


Figure 11 – The effect of offsets with large cell sizes. If the origin is shifted the data may not all reside within a single cell, instead the data is divided into 4 cells. Thus, the declustered mean is not the naïve sample mean.

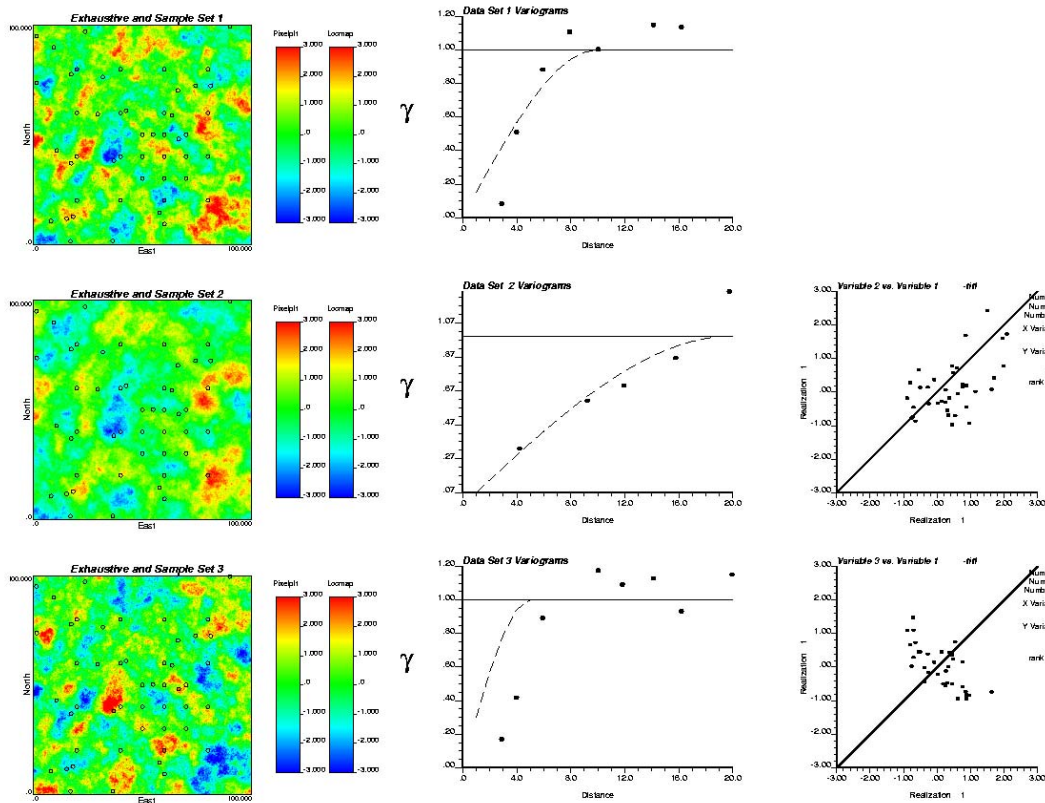


Figure 12 – For each data set, the exhaustive data set with the samples indicated, the variogram model and experimental variogram of the samples and the scatter plot of the samples with the variable 1 samples are shown.

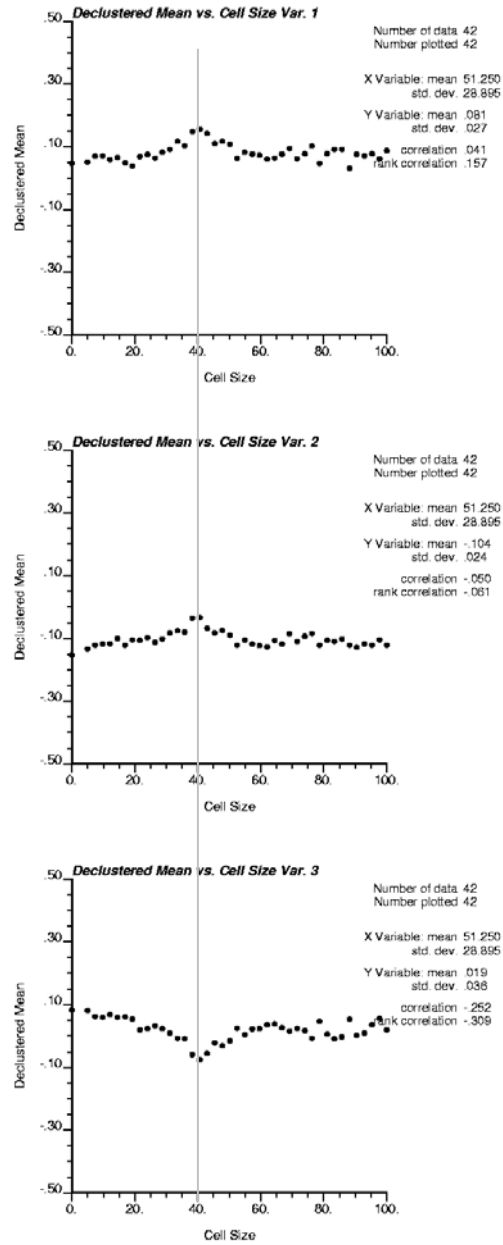


Figure 13 – The declustered mean vs. cell size for the three variables.

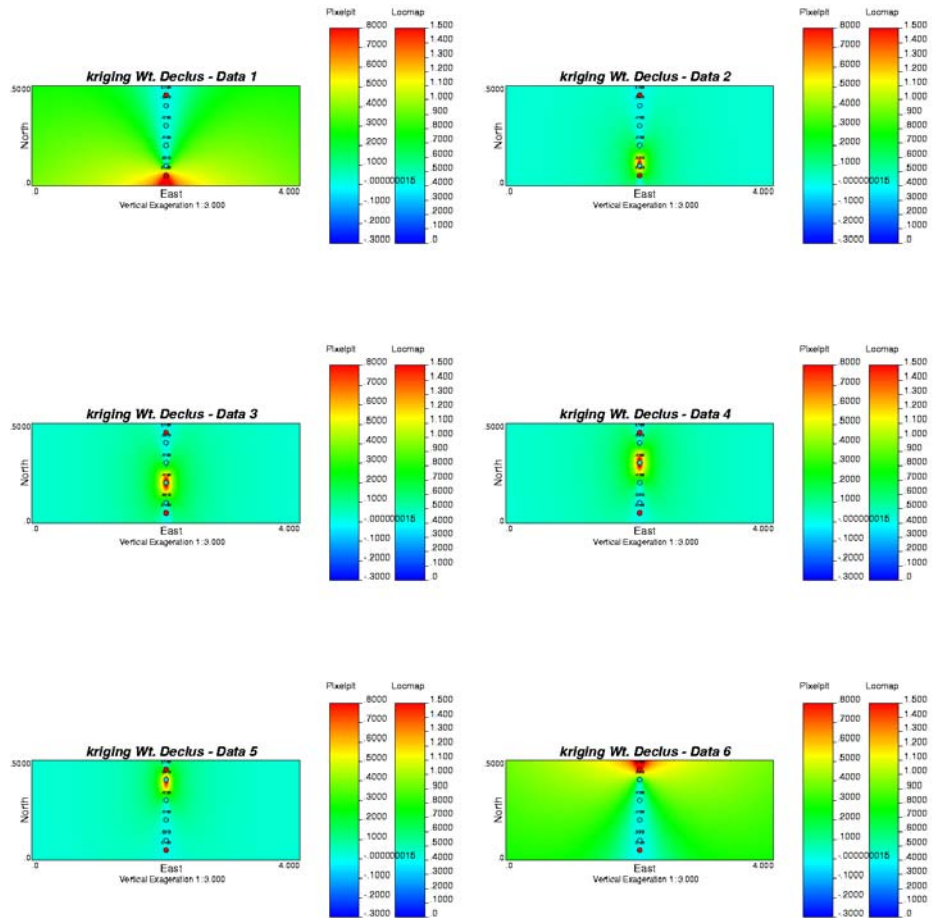


Figure 14 – A string of data, with weights from the kriging weight declustering method indicated, superimposed on the maps of the weights assigned to each data at all locations. The string effect causes the outer data to receive greater weight (see maps for Data 1 and 6).

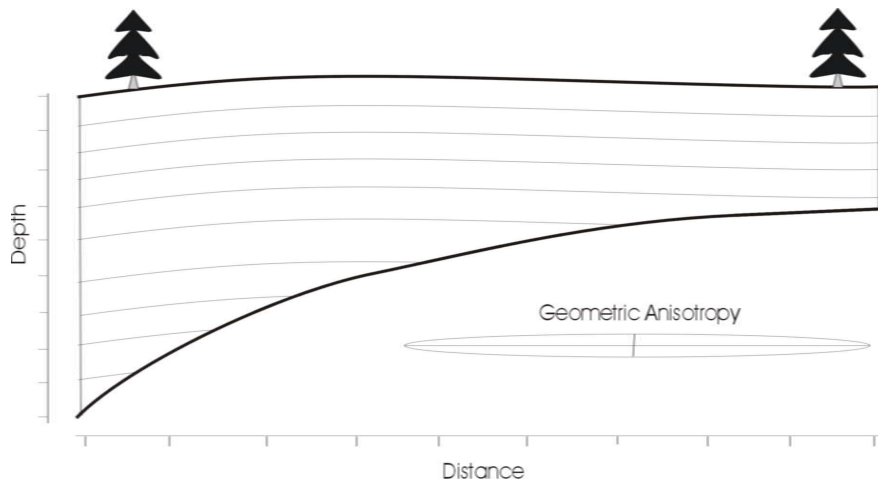


Figure 15 – An example cross section with strong anisotropy.

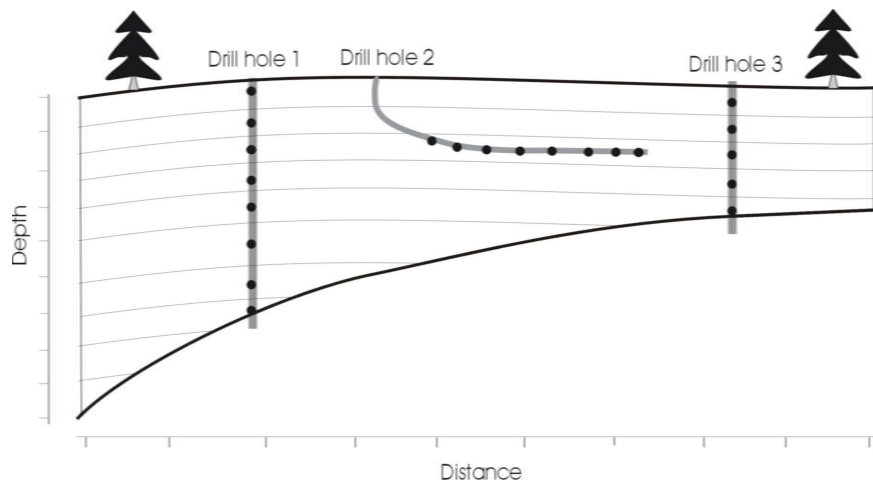


Figure 16 – An example cross section with wells and sample locations.

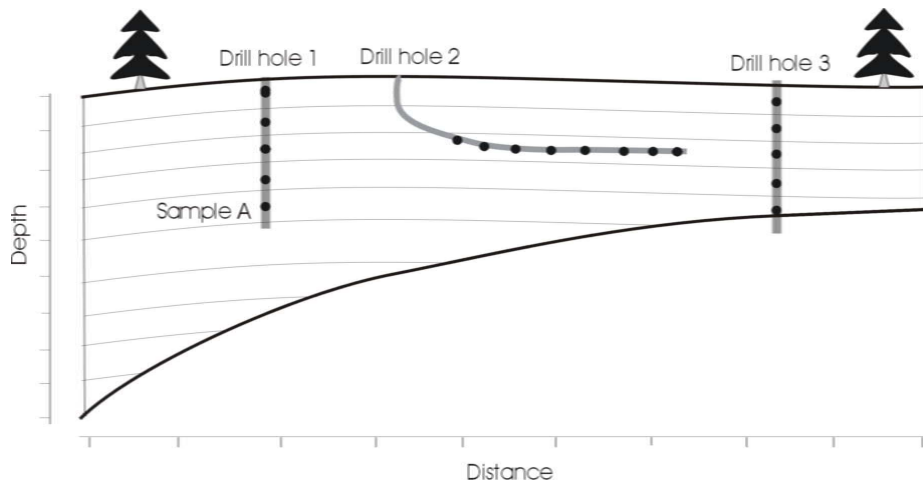


Figure 17 - An example cross section with wells and sample locations.

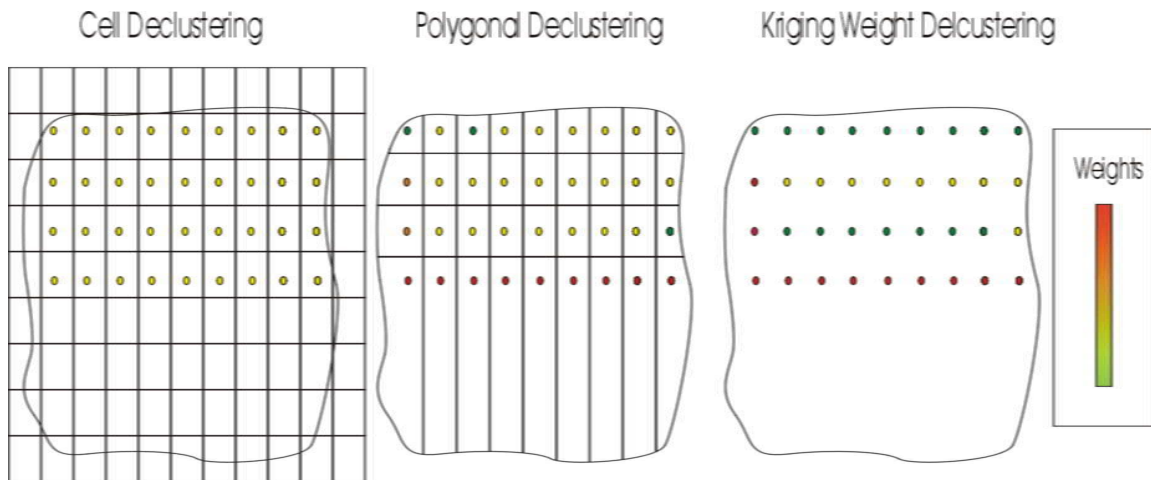


Figure 18 – An illustration of the difference in weight assignments due to a boundary for cell, polygonal and kriging weight declustering. Cell declustering would equally weight the data, while polygonal would larger weight to the data near the unsampled area. Kriging weight declustering would result in weights similar to polygonal, but subject to screening and string effects.

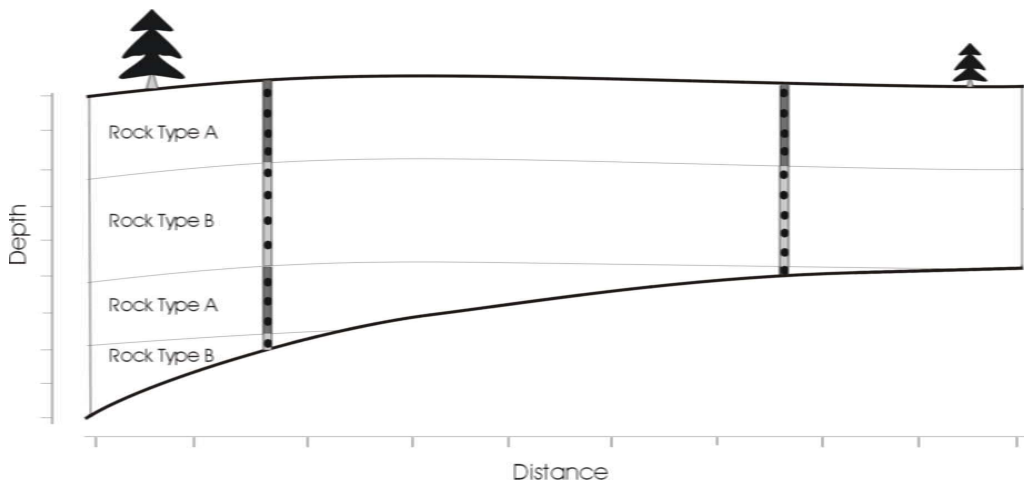


Figure 19 – An example rock type model.

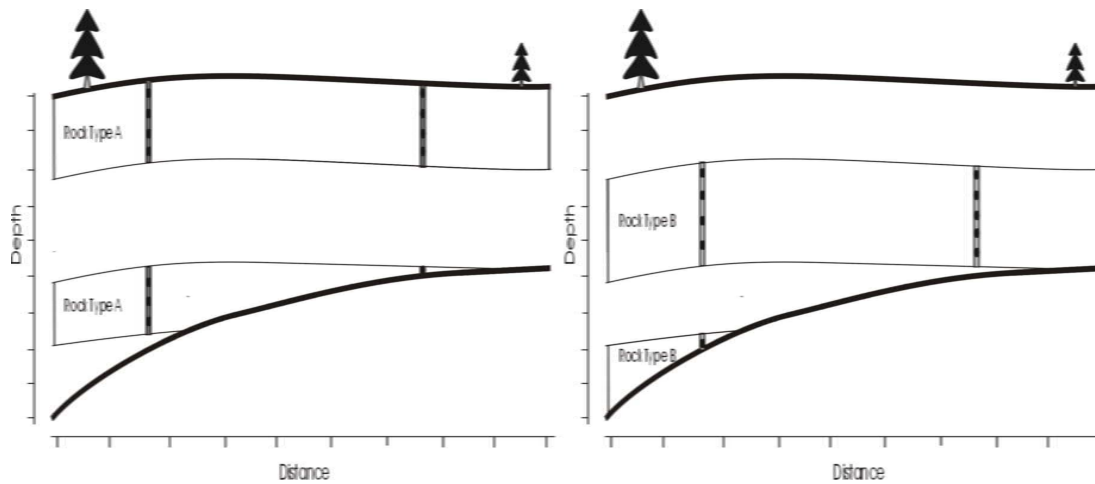


Figure 20 – An example model broken up into separate rock types.

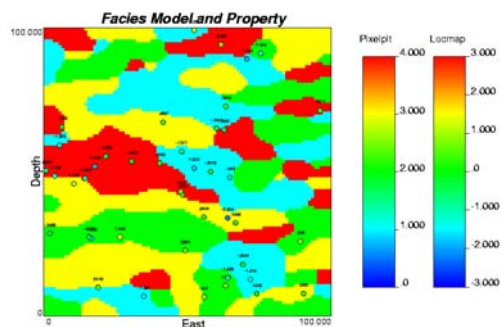


Figure 21 – An example data set and facies model.

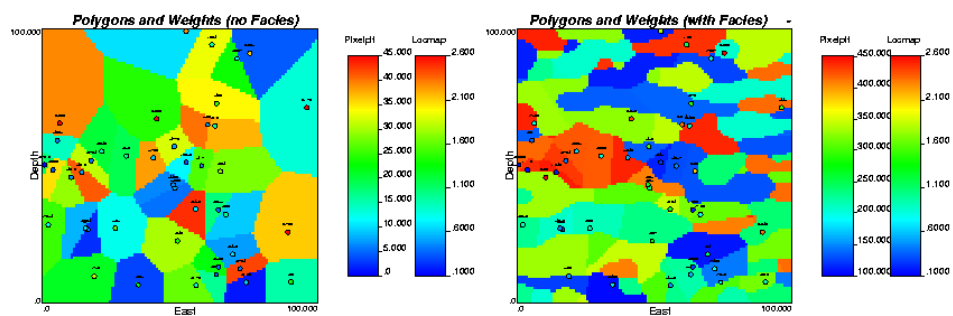


Figure 22 – Polygonal declustering weights and polygons, with and without facies.

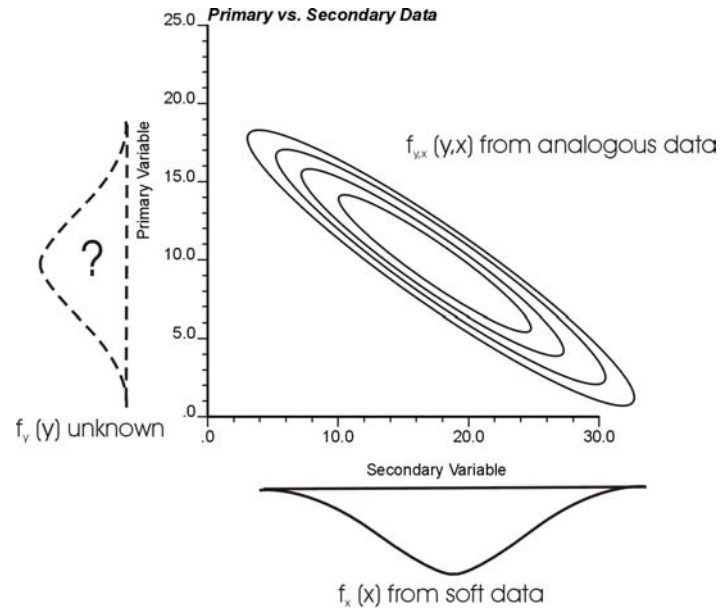


Figure 23 - The calibration bivariate distribution, $\hat{f}_{x,y}(x,y)$, and known marginal distribution of the soft data variable, $f_x(x)$.

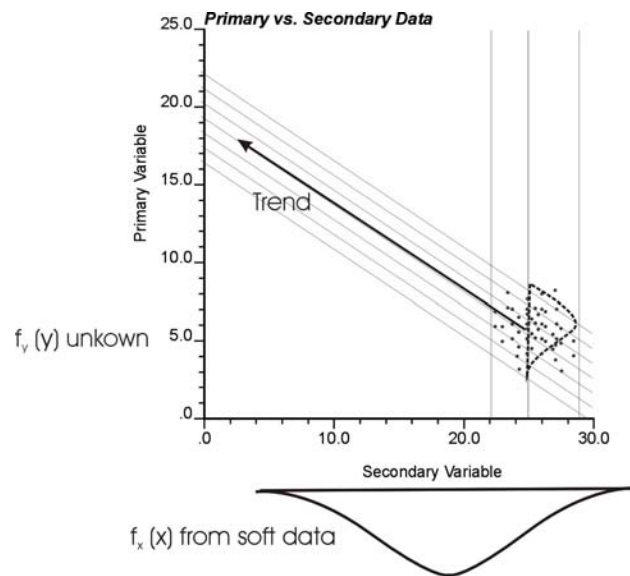


Figure 24 - Calibration by bivariate trend. The points indicate the known primary and secondary data. The arrow indicates a linear bivariate trend. The lines represent probability contours.

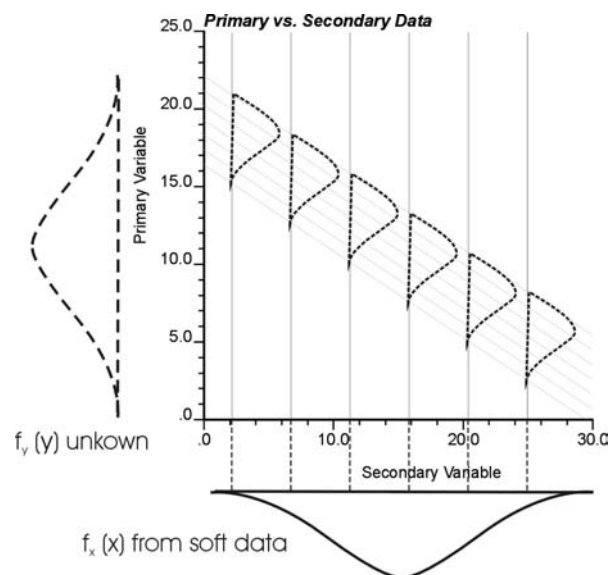


Figure 25 An illustration of the numerical integration of the conditional distribution along the previously indicated linear bivariate trend.

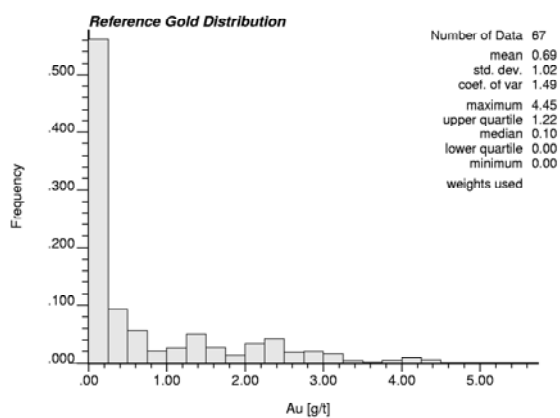


Figure 26 – An approximation of the underlying distribution calculated by polygonal declustering of the complete “red” data set.

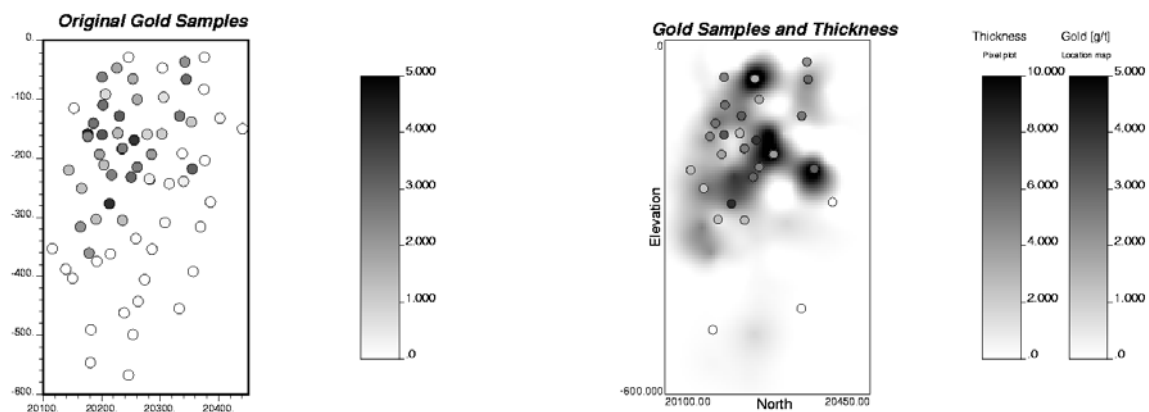


Figure 27 – The original red.dat database (on the left) and the modified data base with kriged thickness map.

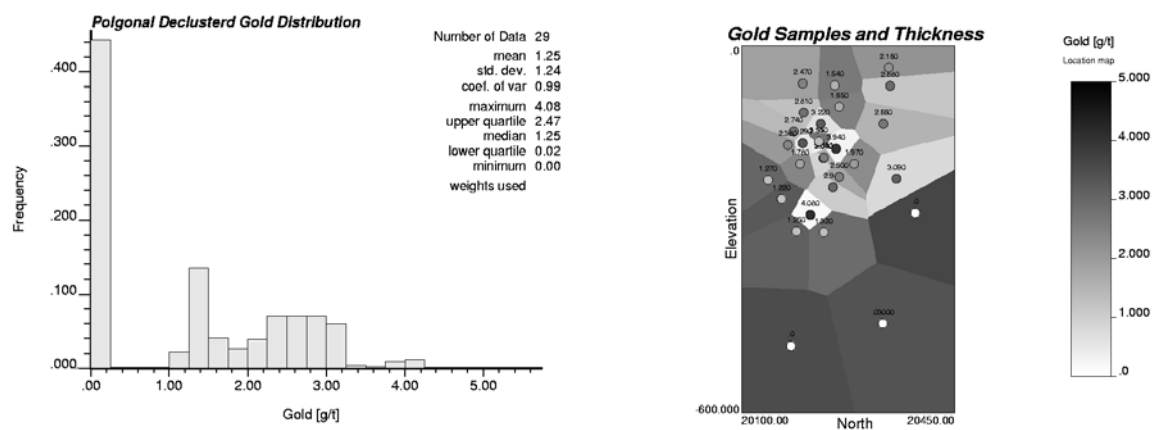


Figure 28 – The resulting distribution from polygonal declustering of the modified red.dat data set and a location map of the data set, with the associated vousior polygons.

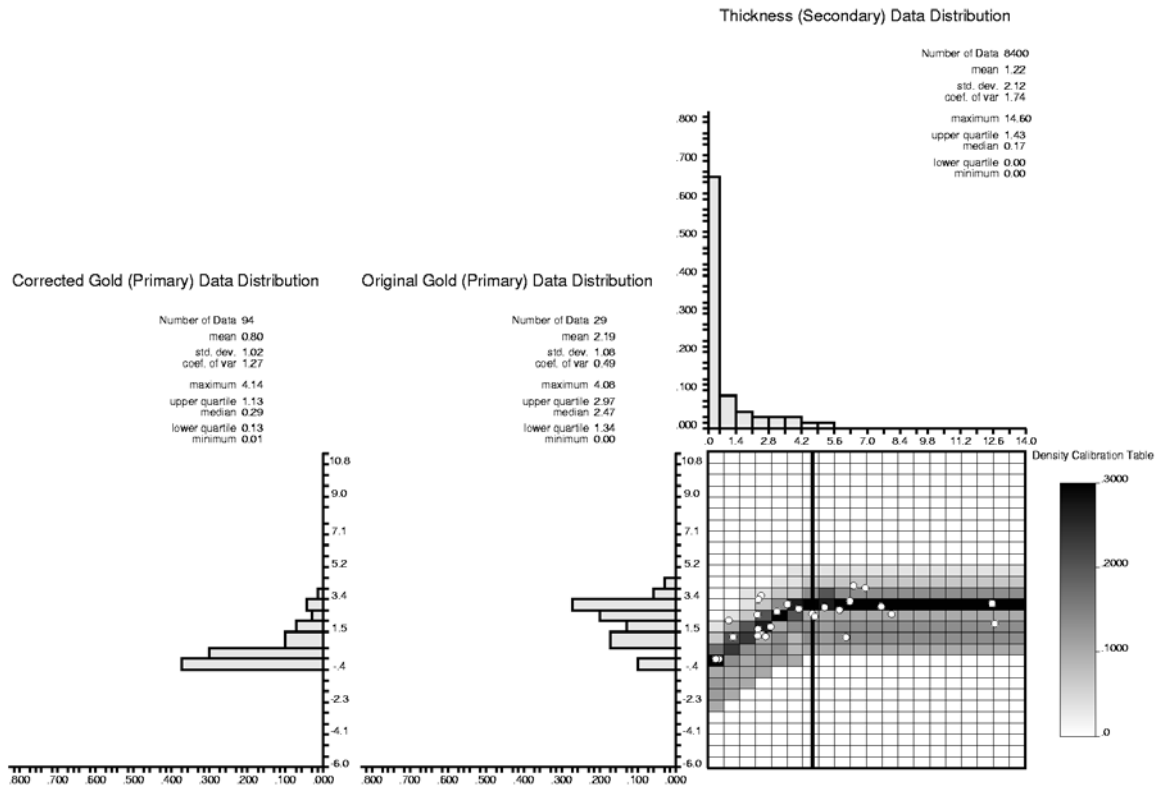


Figure 29 – The density calibration table with collocated thickness data, the thickness distribution, original gold distribution and the corrected gold distribution

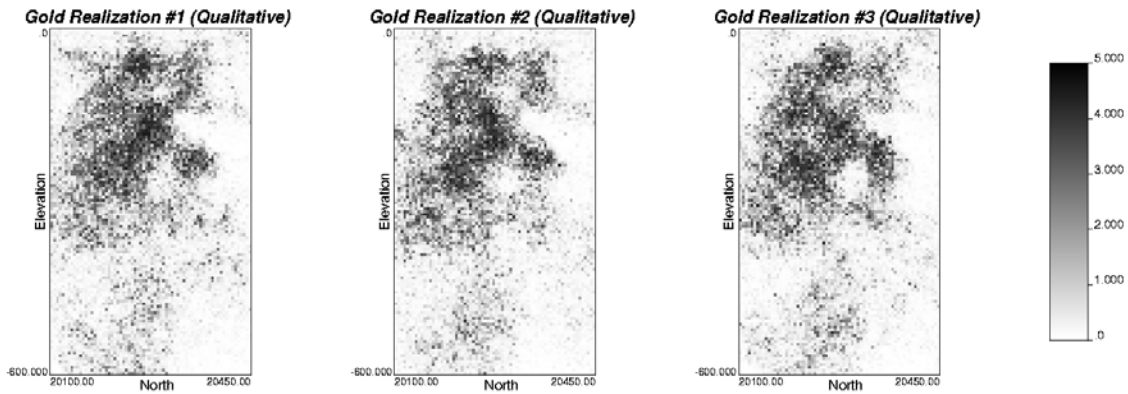


Figure 30 – Three realizations of gold grade using the debiased distribution and collocated thickness (secondary) data.

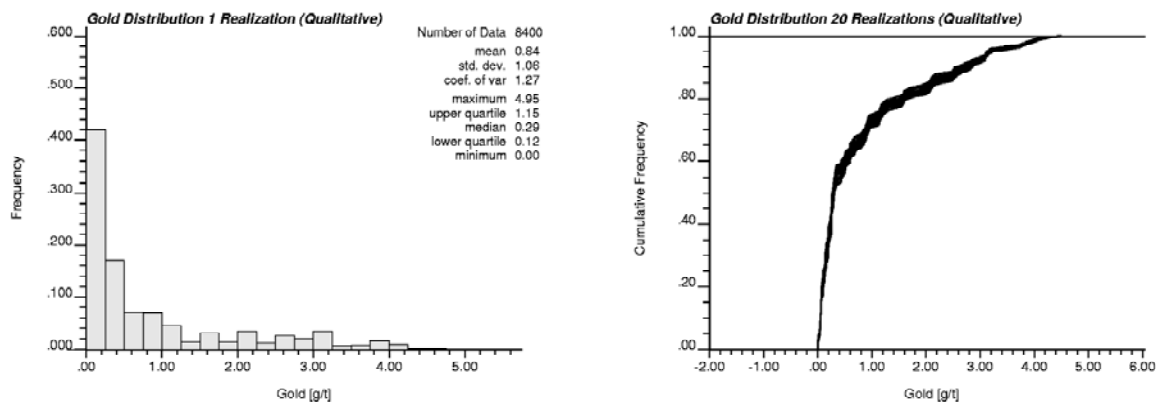


Figure 31 – The histogram of one realization and the cumulative distribution of 20 realizations.

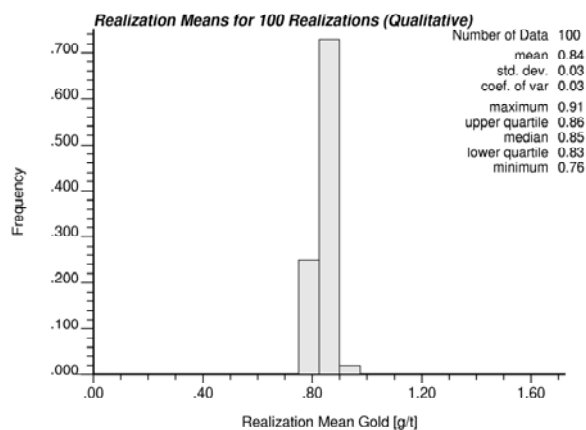


Figure 32 – The histogram of realization means for 100 realizations.

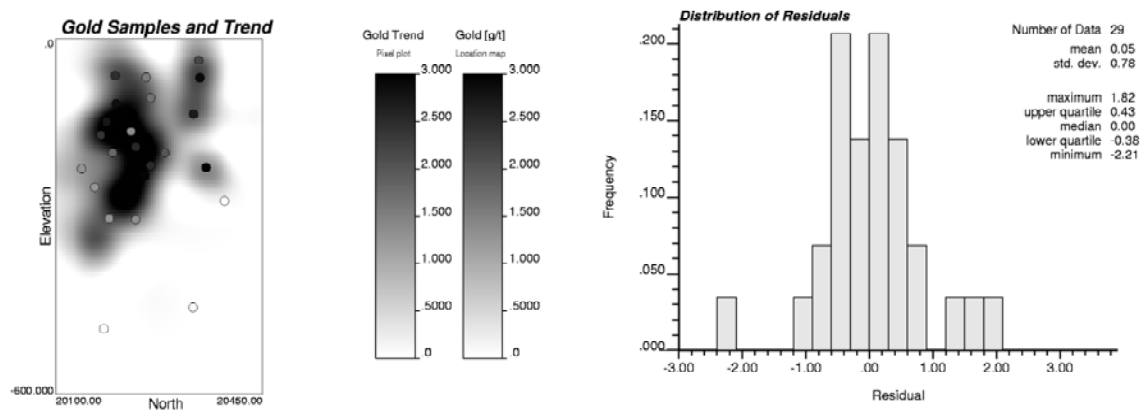


Figure 33 – The reduced “red” data set with a gold trend, and the distribution of the residuals at the data locations.

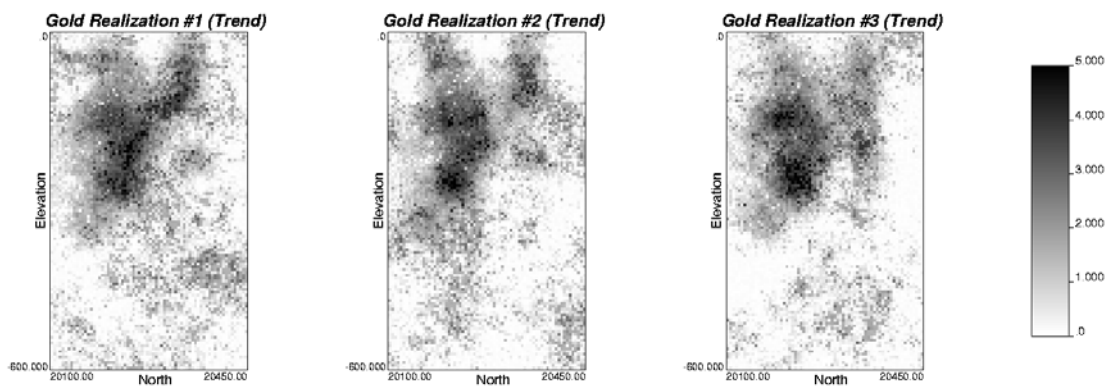


Figure 34 – Three realizations of gold grade resulting from addition of a stochastic residual and a deterministic trend model.

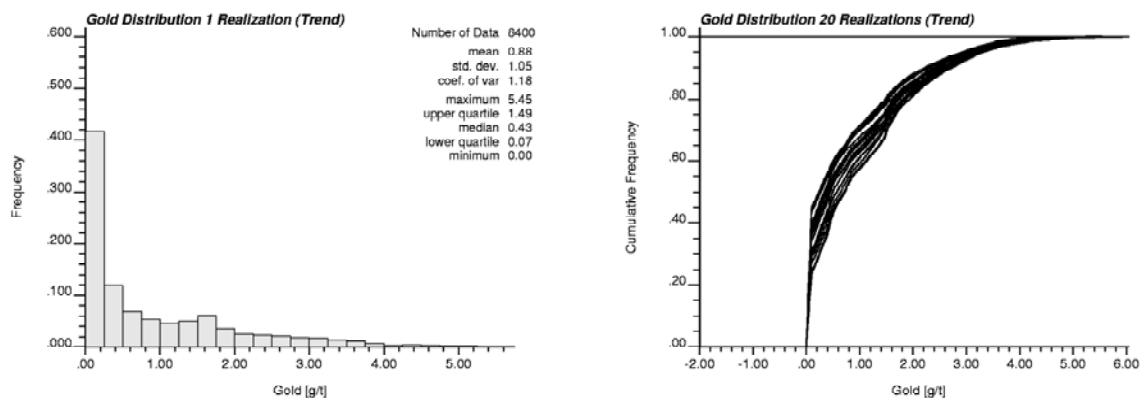


Figure 35 – The histogram of one realization and the cumulative distribution of 20 realizations.

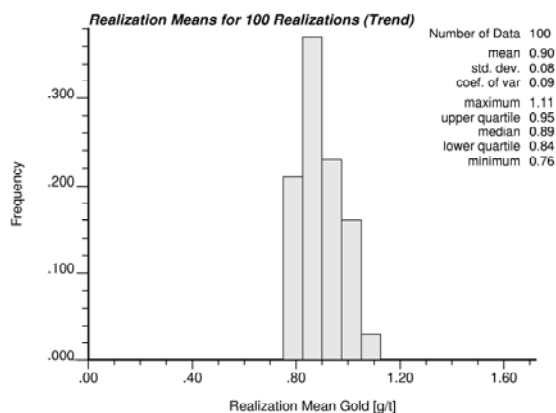


Figure 36 – The histogram of realization means for 100 realizations.